Effect of rapid thermal annealing on recombination centres in boron-doped Czochralski-grown silicon

D. C. Walter,[1,a)] B. Lim,[1] K. Bothe,[1] V. V. Voronkov,[2] R. Falster,[2] and J. Schmidt[1]
[1]*Institute for Solar Energy Research Hamelin (ISFH), Am Ohrberg 1, 31860 Emmerthal, Germany*
[2]*SunEdison, Via Nazionale 59, 39012 Merano, Italy*

(Received 20 November 2013; accepted 15 January 2014; published online 31 January 2014)

Rapid thermal annealing in a belt furnace results in a dramatic change of the recombination properties of boron-doped Czochralski silicon: (1) the lifetime degraded by applying a prolonged illumination at room temperature was significantly improved, (2) after subsequent dark recovery, the lifetime has a remarkably high value, and (3) the permanent recovery, by annealing at 185 °C under illumination, is enormously accelerated, and the finally achieved stable lifetime acquires a record value of 1.5 ms, as compared to 110 μs after permanent recovery of not-annealed reference samples. © *2014 AIP Publishing LLC*. [http://dx.doi.org/10.1063/1.4863674]

In oxygen-rich and boron-doped Czochralski-grown silicon (Cz-Si) that is commonly used for the fabrication of crystalline silicon solar cells, illumination, or injection of excess carriers leads to a severe reduction of the carrier lifetime.[1] Over the last 40 years, this phenomenon has been studied intensively and it had been found that the magnitude of degradation seems to be related to the simultaneous presence of boron and oxygen in the Cz-Si material.[2,3] However, the composition and the kinetics of the boron-oxygen-related recombination defect are still not unambiguously understood. The B-O defect still poses a fundamental limitation on the efficiency of solar cells fabricated of oxygen-rich boron-doped silicon. It has been known for a while that sample cooling after a high temperature process is critical for the B-O defect concentration,[4] although no detailed study on this effect has been performed up to now. In this work, we systematically vary the cooling rate after high-temperature annealing and measure its influence on the lifetime of boron-doped Cz-Si samples in different well-defined states: (i) after complete light-induced degradation, (ii) after subsequent recovery in darkness at 200 °C, and (iii) after permanent recovery.[5]

The material used for this investigation is 150 μm thick boron-doped Cz-Si wafers of a resistivity $\rho = (1.02 \pm 0.03)$ Ω cm and of an interstitial oxygen concentration $[O_i] = (6.9 \pm 0.3) \times 10^{17}\,cm^{-3}$, determined via four-point-probe and FTIR measurements (IOC 88), respectively. Sample processing includes the removal of surface damage, a phosphorus diffusion (850 °C, 1:10 h) followed by the removal of the n^+-region, and the passivation of the surfaces. For the surface passivation, Al_2O_3 is chosen (film thickness 10 nm) which is deposited via plasma-assisted atomic layer deposition (plasma-ALD). A 70 nm thick silicon nitride capping layer is deposited via plasma-enhanced chemical vapour deposition (PECVD) in order to improve the thermal stability of the passivation.[6] The surface passivation of the deposited layers is then activated by annealing at 425 °C for 15 min.[7] On a second sample set, the n^+-region remains on the samples during the rapid thermal annealing (RTA) process. The n^+-region is removed afterwards and the surfaces are passivated with a single Al_2O_3 layer followed by the activation anneal as mentioned above.

The RTA process is carried out in a commercially available belt firing furnace (DO-FF-8.600-300, Centrotherm). In order to realize various cooling rates, different temperature profiles are chosen, corresponding to different belt speeds and peak temperatures. The set peak temperature was either 650 °C or 850 °C and the belt speed was varied from 1.2 m/min up to 7.2 m/min. The temperature profile was monitored by a temperature probe attached to a wafer, which was processed identically to the lifetime samples. The profile is recorded using a *DATAPAQ Insight Oven Tracker*.

Lifetimes are measured using a WCT-120 lifetime tester (Sinton Instruments). If not mentioned, all lifetimes are reported at an injection level of $\Delta n = 0.1 \times p_0$ with Δn being the excess electron concentration and p_0—the dark value of the hole concentration (identical, in our case, to the boron concentration). The characteristic lifetimes are denoted as

(i) τ_d-fully degraded value after light soaking under a halogen lamp at a light intensity of P ≈ 10 mW/cm^2 for 12 h;
(ii) τ_0-after annealing in the dark at 200 °C for 10 min (this lifetime is used as the reference value for calculating the effective concentration of the degrading recombination centres);
(iii) τ_{0p}-after annealing the degraded samples at 185 °C under illumination with a halogen-lamp intensity of 100 mW/cm^2 [this is the stable (permanently recovered) value that does not change (or changes only slightly) upon subsequent illumination at room temperature].

It was found (see Fig. 1) that for all samples these three characteristic lifetimes, τ_0, τ_d, and τ_{0p}, depend critically on the conditions of the RTA process. For both investigated peak temperatures (650 °C and 850 °C), all three lifetimes increase with increasing belt speed. At 850 °C peak temperature and 1.2 m/min belt speed, we measure the lowest lifetimes: $\tau_d = (42 \pm 4)$ μs, $\tau_0 = (107 \pm 3)$ μs, and $\tau_{0p} = (111 \pm 3)$ μs. The lifetime after complete degradation is the highest after the 650 °C RTA treatment with 6 m/min belt speed:

a)Email: d.walter@isfh.de, Tel.: +49 5151 999 424, Fax: +49 5151 999 400

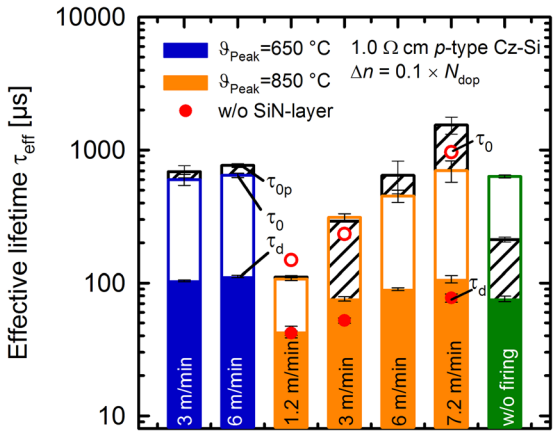

FIG. 1. Measured lifetimes after light soaking τ_d (full columns), after annealing in the dark (200 °C for 10 min) τ_0 (open columns with colour edge), and after permanent recovery τ_{0p} (hatched columns). Orange columns correspond to a peak temperature of 850 °C and blue columns to a peak temperature of 650 °C. Red circles corresponds to the lifetimes τ_d (full symbols) and τ_0 (open symbols) of samples without SiN-layer during RTA treatment. The belt speeds are displayed within each bar. The green column on the right corresponds to samples without additional RTA treatment previous to the lifetime measurement.

$\tau_d = (112 \pm 2)$ µs. The lifetimes after dark recovery and after permanent recovery are the highest after the 850 °C RTA treatment at the maximum belt speed of 7.2 m/min: $\tau_0 = (700 \pm 125)$ µs and $\tau_{0p} = (1540 \pm 225)$ µs. For comparison, the samples without RTA treatment show $\tau_d = (76 \pm 4)$ µs, $\tau_0 = (635 \pm 20)$ µs, and $\tau_{0p} = (212 \pm 9)$ µs; the permanently recovered value is essentially lower than for the RTA-processed samples. Please note that the lifetimes τ_0 and τ_d of the samples without additional hydrogen-rich diffusion barrier also increase with increasing belt speed (red circles in Fig. 1). This indicates that the observed increase of the lifetimes is not due to a hydrogen-related effect, as it was recently suggested by Hallam *et al.*[8] In the following, results of lifetime samples with hydrogen-rich diffusion barriers present during RTA (i.e., Al_2O_3/SiN stacks) are discussed only.

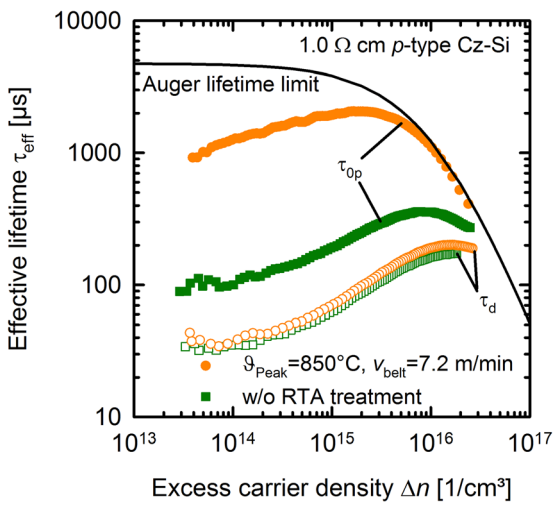

FIG. 2. Measured injection-dependent lifetimes in two different stable states: (i) after complete degradation τ_d and (ii) after permanent recovery τ_{0p}. Open symbols correspond to the lifetimes after complete degradation and closed symbols after permanent recovery. The lifetime values of the sample without RTA treatement are shown as green squares, whereas the lifetimes of the sample with the RTA treatment at 7.2 m/min belt speed and 850 °C peak temperature are shown as orange circles. For comparison, the Auger lifetime limit[9] is also included.

Figure 2 shows the injection level dependence of τ_d (after complete degradation) and τ_{0p} (after permanent recovery) for a reference sample without RTA and a sample after the most efficient RTA treatment (7.2 m/min belt speed and 850 °C peak temperature). While the lifetime curves of τ_d almost coincide, the lifetime τ_{op} is significantly higher for the RTA-processed sample.

The typical change in lifetime during the process of permanent recovery is shown in Fig. 3. The measured lifetimes are transformed into an effective defect concentration $N_t^* = 1/\tau(t) - 1/\tau_0$. The recovery rate constant R_{de} is determined by fitting the $N_t^*(t)$ function by an exponential dependence $A \exp(-R_{de} \times t) + B$. The lowest rate constant, $R_{de} = (1 \pm 0.2)$ h^{-1} (not shown in Fig. 3) was obtained for the sample that had not received any RTA treatment. By applying a peak temperature of 850 °C and a belt speed of 7.2 m/min, R_{de} was increased by almost two orders of magnitude, up to $R_{de} = (75 \pm 11)$ h^{-1}. We thus observe an acceleration of the permanent recovery process by two orders of magnitude after the RTA treatment and an increase of the absolute lifetime after permanent recovery of one order of magnitude.

In a recent defect model,[10] the reduction of the effective lifetime upon light soaking has been attributed to a change in the configuration of a grown-in complex consisting of an interstitial boron atom (B_i) and an oxygen dimer (O_2). During cooling, the free interstitial boron atoms (produced by self-interstitials emitted by oxide particles) agglomerate into small precipitates (nano-precipitates, NPs). This happens at a relatively high temperature deduced below to be around 600 °C. At this stage, the remaining free interstitial boron atoms are in equilibrium with the NPs, and there are also complexes of B_i with other impurities, such as B_s, O, O_2, etc. The defect responsible for the light-induced degradation has been proposed to be B_iO_2. Below some relatively low characteristic temperature ϑ_f (roughly, less than 350 °C), the

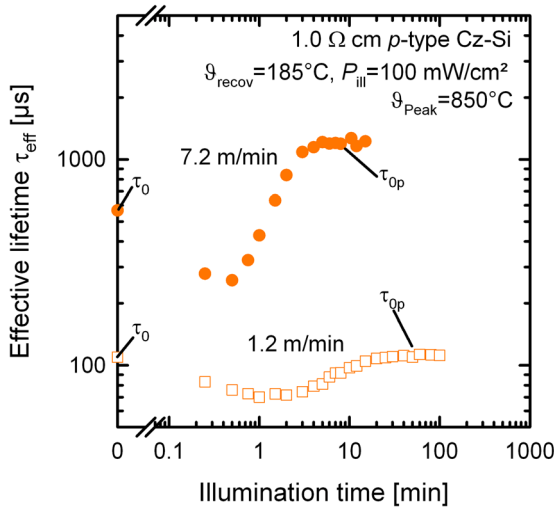

FIG. 3. Measured effective lifetime during the process of permanent recovery. Circles correspond to a sample processed at 7.2 m/min belt speed; squares correspond to a sample processed at 1.2 m/min belt speed during RTA.

equilibrium between the B_i-containing defects and the NPs is no longer supported, and the total concentration of these defects is frozen-in. This means that the concentration of frozen-in B_iO_2 defects depends on the cooling rate $q = -d\vartheta/dt$ referring to ϑ_f, and also on the NP density and size—which in turn depend on q but now referring to a different characteristic temperature ϑ_n.[10,11] Besides, the concentration of oxygen dimers is also frozen-in at its own characteristic temperature, and hence depends on the cooling rate referring to that temperature. Accordingly, the dependence of the frozen-in B_iO_2 concentration (and hence of the degraded lifetime τ_d) on the cooling conditions is somewhat complicated being dependent on the full cooling curve rather than on the cooling rate within a definite temperature interval. A noticeable impact of sample cooling after a high temperature step on the effective defect concentration N_t* was reported previously by Bothe *et al.*[4]

The permanent recovery can be attributed to increasing the free B_i atom concentration by a partial dissociation of B_i-containing complexes at elevated temperature and in the presence of excess carriers. An enhanced loss of B_i to the NPs[10,12] leads to the disappearance of all B_i-containing centres—including B_iO_2—and subsequent illumination at room temperature does not lead to a renewed lifetime degradation. The rate constant of the permanent recovery R_{de} is then proportional to the sinking ability of NPs, which is characterized by the product of the NP density N_p and the average NP radius R_p as discussed in detail in Ref. 12. These properties of the NPs can be analyzed by an analogy with vacancy aggregation into voids.[13] Upon lowering ϑ, the nucleation rate of NPs is fast increasing, and, at some moment, becomes so high that the number of growing NPs consumes the dissolved B_i, thus suppressing further nucleation. Appreciable nucleation occurs within a very narrow temperature interval, and the produced NP density N_p and the final radius R_p (upon consuming majority of dissolved B_i) depend in a simple way on the cooling rate q and on the concentration C_i of B_i atoms prior to the nucleation/growth stage. Remarkably, the quantity of interest, the $N_p \times R_p$ product, is independent of C_i and simply proportional to q. Hence, the rate constant for the permanent recovery (deactivation) should follow this simple dependence on the cooling rate,

$$R_{de} \sim N_p \times R_p \sim q. \quad (1)$$

The cooling rate q in this expression refers to a narrow temperature interval where the NP nucleation occurs and thus to some definite temperature ϑ_n of nucleation—which is unknown beforehand but can be estimated by the present data. To do so, we determine the cooling rate of every investigated temperature profile within specific temperature intervals using linear approximations. We find a linear correlation of R_{de} and $q = -d\vartheta/dt$ for the temperature range 575–625 °C, as can be seen in Fig. 4. It is then concluded that the nucleation temperature of NPs is around 600 °C. The highest achieved recovery rate constant, $R_{de} = (75 \pm 11)\ h^{-1}$, corresponds to a cooling rate $q = 100$ °C/s within the indicated temperature range. It is expected that further increasing the cooling rates (although difficult to realize experimentally) would lead to still higher values of R_{de}. The proportionality

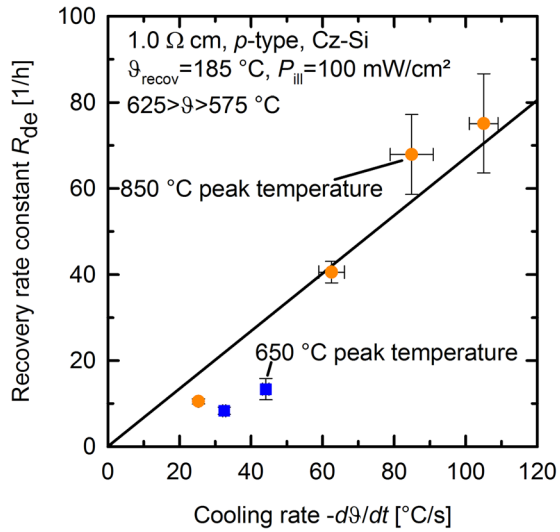

FIG. 4. Measured recovery rate constant R_{de} as a function of the cooling rate $-d\vartheta/dt$ in a temperature range between 575 °C and 625 °C. Samples with RTA treatment at 850 °C peak temperature are shown as orange circles; samples with RTA treatment at 650 °C are shown as blue squares. The black line is a guide to the eye.

coefficient between R_{de} and q (with the units used above) is about 2.08×10^{-4} °C^{-1}.

The majority of B_i-containing complexes is believed to disappear in the course of permanent recovery. The achieved lifetime τ_{0p} is controlled by some other point defects. In principle, also the NPs may contribute into the recombination but this contribution is apparently very small—since the highest value of τ_{0p} is observed for the highest cooling rate, when the NP density is the highest.

The effective concentration after complete degradation, $N_d^* = 1/\tau_d - 1/\tau_0$, is proportional to the frozen-in concentration of B_iO_2 and hence should depend on the cooling conditions in a more complicated way—as discussed above—being sensitive to the entire cooling curve. In Fig. 5, N_d* is plotted in dependence of only one cooling rate—referring to the

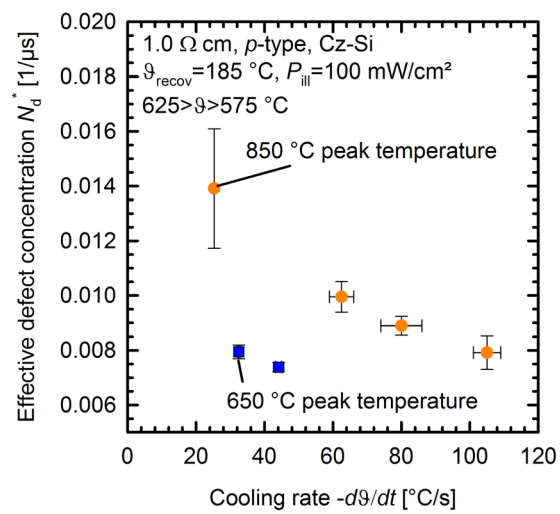

FIG. 5. Effective defect concentration N_d* plotted versus the cooling rate $-d\vartheta/dt$ in a temperature range between 525 and 625 °C. Samples with RTA treatment at 850 °C peak temperature are marked in orange circles; samples with RTA treatment at 650 °C are marked with blue squares. N_d* decreases with increasing cooling rate.

temperature interval of 625–575 °C. There is a well pronounced reduction in N_d* upon increasing the cooling rate, although the effect is not as strong as for the permanent recovery rate constant R_{de}.

In this Letter, we have examined the impact of rapid thermal annealing, performed in a belt-type firing furnace as used for the metallization of screen-printed silicon solar cells, on the carrier lifetime of boron-doped oxygen-rich *p*-type Cz-Si wafers, for some characteristic stages of light-induced degradation/recovery. By varying the peak temperatures and the cooling rates of the RTA treatment, significant differences in the lifetimes after complete degradation (τ_d), after dark annealing (τ_0), and after permanent recovery (τ_{0p}) were observed. Using the same Cz-Si material, we have found that the degraded lifetime can be improved by RTA from 42 μs to 107 μs. The permanently recovered lifetime can be improved much more dramatically: from 110 μs to 1540 μs. We also observed a very strong impact of the RTA treatment on the kinetics of the permanent recovery. Due to the RTA, the recovery rate constant R_{de} was increased from 1 h^{-1} to 75 h^{-1} for the highest applied belt speed of 7.2 m/min and, accordingly, the highest cooling rate of about 100 °C/s in the relevant temperature interval, which was deduced to be around 600 °C. We observed a linear increase of the recovery rate constant with increasing cooling rate $R_{de} \sim -d\vartheta/dt$, taken in this temperature interval. The present experimental findings are treated within a previously proposed B_iO_2 model for the lifetime-degrading recombination centres.[10] In this model, various B_i-containing complexes exist—in the initial stage of sample cooling from a high ϑ—in equilibrium with the boron NPs but at lower temperature the equilibrium is no longer supported, and some concentration of B_iO_2 is frozen-in. This concentration is expected to be smaller at higher cooling rate. The sinking ability of the NPs (the product of their density and the radius) is predicted to be simply proportional to the cooling rate referring to a specific temperature of NP nucleation. We have concluded that this nucleation temperature is around 600 °C. The rate constant for the permanent recovery is proportional to the NP sinking efficiency—and thus to the cooling rate.

[1]Fischer and W. Pschunder, in *Proceedings of the 10th IEEE Photovoltaic Specialists Conference, Palo Alto, CA* (IEEE, New York, 1973), p. 404.
[2]J. Schmidt, A. G. Aberle, and R. Hezel, in *Proceedings of the 26th IEEE Photovoltaic Specialists Conference, Anaheim, CA* (IEEE, NewYork, 1997), p. 13.
[3]S. W. Glunz, S. Rein, W. Warta, J. Knobloch, and W. Wettling, in *Proceedings of the 2nd World Conference on Photovoltaic Solar Energy Conversion, Vienna, Austria* (WIP, Munich, 1998), p. 1343.
[4]K. Bothe, J. Schmidt, and R. Hezel, in *Proceedings of the 29th IEEE Photovoltaic Specialists Conference, New Orleans, LA* (IEEE, New York, 2002), p. 194.
[5]A. Herguth, G. Schubert, M. Kaes, and G. Hahn, in *Proceedings of the 21st European Photovoltaic Solar Energy Conference, Dresden, Germany* (WIP, Munich, 2006), p. 530.
[6]J. Schmidt, B. Veith, and R. Brendel, Phys. Status Solidi RRL **3**, 287–289 (2009).
[7]F. Werner, B. Veith, V. Tiba, P. Poodt, F. Roozeboom, R. Brendel, and J. Schmidt, Appl. Phys. Lett. **97**, 162103 (2010).
[8]B. J. Hallam, P. G. Hamer, S. R. Wenham, M. D. Abbott, A. Sugianto, A. M. Wenham, C. E. Chan, G. Xu, J. Kraiem, J. Degoulange, and R. Einhaus, IEEE J. Photovoltaics **4**, 88 (2014).
[9]A. Richter, F. Werner, A. Cuevas, J. Schmidt, and S. W. Glunz, Energy Procedia **27**, 88–94 (2012).
[10]V. V. Voronkov and R. Falster, J. Appl. Phys. **107**, 053509 (2010).
[11]R. J. Falster and V. V. Voronkov, U.S. patent application publication 2013/0102129 A1 (25 April 2013).
[12]V. V. Voronkov, R. Falster, B. Lim, and J. Schmidt, J. Appl. Phys. **112**, 113717 (2012).
[13]V. V. Voronkov and R. Falster, J. Cryst. Growth **194**, 76–88 (1998).